Kinematics and trajectory planning of a cucumber harvesting robot manipulator

Zhang Libin, Wang Yan, Yang Qinghua, Bao Guanjun, Gao Feng, Xun Yi

(*The MOE Key Laboratory of Mechanical Manufacture and Automation, Zhejiang University of Technology, Hangzhou* 310012, *China*)

Abstract: In order to reduce cucumber harvesting cost and improve economic benefits, a cucumber harvesting robot was developed. The cucumber harvesting robot consists of a vehicle, a 4-DOF articulated manipulator, an end-effector, an upper monitor, a vision system and four DC servo drive systems. The Kinematics of the cucumber harvesting robot manipulator was constructed using D-H coordinate frame model. And the inverse kinematics which provides a foundation for trajectory planning has been solved with inverse transform technique. The cycloidal motion, which has properties of continuity and zero velocity and acceleration at the ports of the bounded interval, was adopted as a feasible approach to plan trajectory in joint space of the cucumber harvesting robot manipulator. Moreover, hardware and software based on CAN-bus communication between the upper monitor and the joint controllers have been designed. Experimental results show that the upper monitor communicates with the four joint controllers efficiently by CAN-bus, and the integrated errors of four joint angles do not exceed four degrees. Probable factors resulting in the errors were analyzed and the corresponding solutions for improving precision are proposed.

Keywords: cucumber harvesting robot, articulated manipulator, trajectory planning, cycloidal motion, CAN-bus

DOI: 10.3965/j.issn.1934-6344.2009.01.001-007

Citation: Zhang Libin, Wang Yan, Yang Qinghua, Bao Guanjun, Gao Feng, Xun Yi. Kinematics and trajectory planning of a cucumber harvesting robot manipulator. Int J Agric & Biol Eng, 2009; 2(1): 1－7.

1 Introduction

Fruit and vegetable harvesting is a labor-intensive job, and the harvesting cost by human labor is about 33%～50% of the total production cost[1]. Therefore, it is urgent to mechanize and automate fruit and vegetable harvesting. Currently, many countries are studying harvesting robot, especially Netherlands and Japan. Some of the harvesting robots, such as cucumber, tomato, grape harvesting robots have been applied in greenhouses and others on farms[2,3]. In China, though research on harvesting robot is later than that in developed countries, some favorable achievements have been made through efforts in many universities and research institutes, such as the eggplant picking robot designed by China Agricultural University and the tomato harvesting robot developed by Zhejiang University.

Under the support of the National High-Tech Research and Development (863) Program of China (2007AA04Z222), the first systematical cucumber harvesting robot in China was jointly developed by China Agricultural University and Zhejiang University of Technology. It consists of a vehicle, a 4-degree of freedom (DOF for short) articulated manipulator, an end-effector, an upper monitor, a vision system and four DC servo drive systems. Instead of utilizing an industrial

Received date: 2008-11-20 Accepted date: 2009-03-28

Biographies: Zhang Libin, professor, Ph.D, mainly engaged in agricultural robot, mechatronics and control. **Wang Yan,** Ph.D candidate of Zhejiang University of Technology, mainly engaged in robotics, intelligent instruments. **Yang Qinghua,** professor, Ph.D, mainly engaged in robotics, mechatronics and control. **Bao Guanjun,** lecturer, Ph.D, mainly engaged in robotics, control and machine vision. **Gao Feng,** associate professor, Ph.D, mainly engaged in electromechanical engineering. **Xun Yi**, Ph.D, mainly engaged in vision system and image processing.

Corresponding author: Zhang Libin, MOE Key Laboratory of Mechanical Manufacture and Automation, Zhejiang University of Technology, Hangzhou 310012, China. Tel & fax: +86-571-88320007. Email: robot@zjut.edu.cn

manipulator, the 4-DOF articulated manipulator was designed by Zhejiang University of Technology to reduce the cost and adapt to the harvesting environment.

This paper mainly investigates the 4-DOF articulated manipulator kinematics and trajectory planning, and it is outlined as follows. In Section 1, the structure of cucumber harvesting robot manipulator is described. The kinematics of manipulator is constructed in Section 2 and the inverse kinematics is solved in Section 3. Section 4 presents the trajectory planning algorithm of cycloidal motion. The hardware and software design of trajectory planning based on CAN-bus is introduced in Section 5. Experiments measuring actual position of four joints are carried out and possible causes for errors are analyzed in Section 6. Finally, conclusions are drawn in Section 7.

2 Cucumber harvesting robot manipulator structure

This paper describes in detail the kinematics of the robot manipulator and realization of trajectory planning control based on CAN-bus. The line diagram and photograph of the articulated manipulator is shown in Figure 1. It is composed of four rotation joints: waist joint (J1), shoulder joint (J2), elbow joint (J3) and wrist joint (J4). One end is fixed on the base, and the other end is connected to an end-effector which contains two parts: a gripper to grasp the fruit and a cutting device to separate the fruit from the plant.

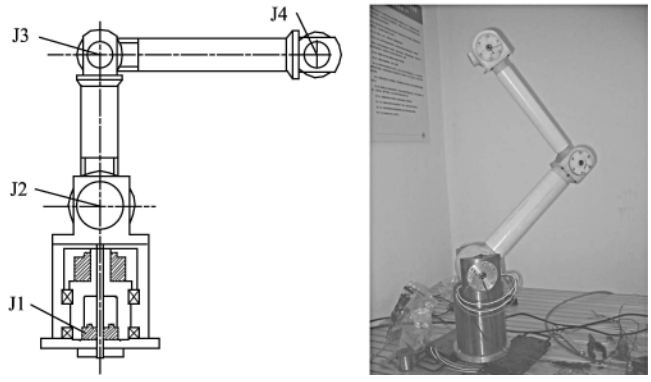

Figure 1 Line diagram and photograph of the cucumber harvesting robot manipulator

The cucumber harvesting robot system employs multi-CPU, distributed control structure of upper monitor and joint servo controllers. Moreover, the four joints are driven to work in perfect harmony by CAN-bus communication which efficiently supports the distributed real-time control system. The communication system of the cucumber harvesting robot is shown in Figure 2. The Upper monitor is used to monitor and manage the whole robot system, locate cucumber target, and plan trajectory. The CAN-bus is the transmission bridge between upper monitor and joint controllers. The servo controllers are distributed in each joint to drive torque motors and they can realize close-loop control by receiving feed back signals from angle encoders.

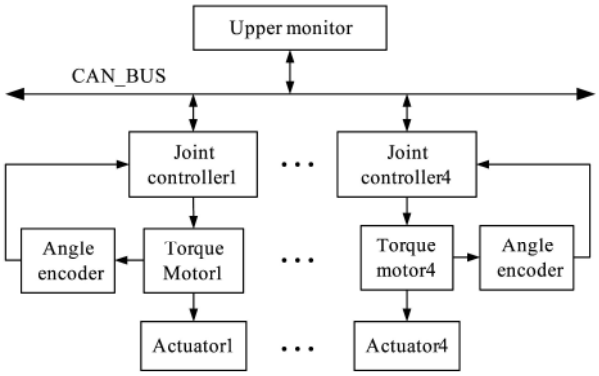

Figure 2 Communication system of the cucumber harvesting robot

3 Coordinate frames of kinematics models

Coordinate frames of kinematics models are constructed by Denavit-Hartenberg model (D-H for short), which has been widely adopted in robotics due to its explicit physical interpretation of mechanisms and relatively easy implementation in the programming of the robot manipulator. D-H coordinate frame model is based on assignment of Cartesian coordinate frames fixed relative to each link of robot manipulator. And it describes spatial transformation between two consecutive links by 4×4 transformation matrix ${}^{i-1}A_i$, so the transformation of link n coordinate frame into the base coordinate frame can be written as[4,5]:

$$ {}^{0}A_n = {}^{0}A_1\,{}^{1}A_2 \ldots {}^{n-1}A_n = \begin{bmatrix} n_x & o_x & a_x & p_x \\ n_y & o_y & a_y & p_y \\ n_z & o_z & a_z & p_z \\ 0 & 0 & 0 & 1 \end{bmatrix} = \begin{bmatrix} \boldsymbol{n} & \boldsymbol{o} & \boldsymbol{a} & \boldsymbol{p} \\ 0 & 0 & 0 & 1 \end{bmatrix} \quad (1) $$

where $\boldsymbol{a}$ is the vector of approaching direction; $\boldsymbol{o}$ is the orientation vector, $\boldsymbol{n}=\boldsymbol{o}\times\boldsymbol{a}$ is the normal vector; $\boldsymbol{p}$ is the position vector of end-effector relative to the base coordinate frame.

The D-H transformation matrix ${}^{i-1}A_i$ relating to a number of rotations and translations between two consecutive coordinate frames is expressed as[6,7]:

$$ {}^{i-1}A_i=\begin{bmatrix}\cos\theta_i & -\sin\theta_i\cos\alpha_i & \sin\theta_i\sin\alpha_i & a_i\cos\theta_i\\ \sin\theta_i & \cos\theta_i\cos\alpha_i & -\cos\theta_i\sin\alpha_i & a_i\sin\theta_i\\ 0 & \sin\alpha_i & \cos\alpha_i & d_i\\ 0 & 0 & 0 & 1\end{bmatrix} \quad (2)$$

where θ_i is joint angle; α_i is twist angle; d_i is joint offset; a_i is the length of link.

Figure 3 illustrates the D-H coordinate frames of the robot manipulator and Table 1 summarizes its D-H parameters.

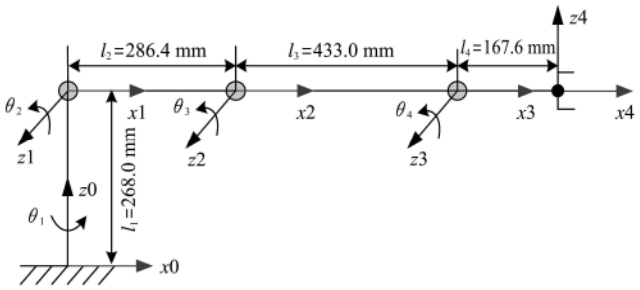

Figure 3 D-H coordinate frames of the cucumber harvesting robot manipulator

Table 1 D-H parameters of the robot manipulator

Link i	α_i /deg	a_i /mm	d_i /mm	θ_i /deg	Joint range /deg
1	90	0	l_1	θ_1	-90~90
2	0	l_2	0	θ_2	0~90
3	0	l_3	0	θ_3	-90~0
4	-90	l_4	0	θ_4	-90~90

4 Inverse kinematics of the cucumber harvesting robot manipulator

The inverse kinematics problem for a robot manipulator is to find a vector of joint variables that produces a desired end-effector position and orientation. The inverse transform technique is used to solve the problem[8,9]. In order to pick cucumbers conveniently, the wrist joint has to be parallel to X axis of the base coordinate frame, so it can be obtained: $\theta_2+\theta_3+\theta_4=0^\circ$

For equation (1), it can be rewritten as:

$$ {}^1A_2\cdot{}^2A_3\cdot{}^3A_4=({}^0A_1)^{-1}\cdot{}^0A_4 \quad (3)$$

$$ {}^1A_2\cdot{}^2A_3\cdot{}^3A_4=\begin{bmatrix}c_{234} & 0 & -s_{234} & l_2c_2+l_3c_{23}+l_4c_{234}\\ s_{234} & 0 & c_{234} & l_2s_2+l_3s_{23}+l_4s_{234}\\ 0 & -1 & 0 & 0\\ 0 & 0 & 0 & 1\end{bmatrix} \quad (4)$$

$$ ({}^0A_1)^{-1}\cdot{}^0A_4=\begin{bmatrix}c_1 & s_1 & 0 & 0\\ 0 & 0 & 1 & -l_1\\ s_1 & -c_1 & 0 & 0\\ 0 & 0 & 0 & 1\end{bmatrix}\cdot\begin{bmatrix}n_x & o_x & a_x & p_x\\ n_y & o_y & a_y & p_y\\ n_z & o_z & a_z & p_z\\ 0 & 0 & 0 & 1\end{bmatrix}$$

$$ =\begin{bmatrix}c_1n_x+s_1n_y & c_1o_x+s_1o_y & c_1a_x+s_1a_y & c_1p_x+s_1p_y\\ n_z & o_z & a_z & p_z-l_1\\ s_1n_x-c_1n_y & s_1o_x-c_1o_y & s_1a_x-c_1a_y & s_1p_x-c_1p_y\\ 0 & 0 & 0 & 1\end{bmatrix} \quad (5)$$

where $s_i=\sin(\theta_i);c_i=\cos(\theta_i);c_{23}=\cos(\theta_2+\theta_3);$ $s_{23}=\sin(\theta_2+\theta_3).$

First, let element (3,4) of matrix (4) and (5) be equal, θ_1 can be given by:

$$ \theta_1=\arctan(p_y/p_x); \quad (6)$$

Then let element (1, 4) and (2, 4) of matrix (4) and (5) be equal, the following equations can be obtained:

$$ \begin{cases}c_1p_x+s_1p_y=l_2c_2+l_3c_{23}+l_4c_{234}=l_2c_2+l_3c_{23}+l_4\\ p_z-l_1=l_2s_2+l_3s_{23}+l_4s_{234}=l_2s_2+l_3s_{23}\end{cases} \quad (7)$$

By simplifying equation (7):

$$ c_3=\frac{(c_1p_x+s_1p_y-l_4)^2+(p_z-l_1)^2-l_3^2-l_2^2}{2l_2l_3} \quad (8)$$

$$ s_3=\pm\sqrt{1-c_3^2} \quad (9)$$

$$ \theta_3=-\arcsin(s_3) \quad (10)$$

From equation (7), θ_2,θ_3 can be expressed as:

$$ c_2=\frac{(l_3c_3+l_2)(c_1p_x+s_1p_y-l_4)+(p_z-l_1)l_3s_3}{(l_3c_3+l_2)^2+l_3^2s_3^2} \quad (11)$$

$$ \theta_2=\arccos(c_2) \quad (12)$$

$$ \theta_4=-(\theta_2+\theta_3) \quad (13)$$

5 Trajectory planning in joint space based on cycloidal motion

Trajectory planning of the robot manipulator is defined in this way: find temporal motion laws for joint position, velocity and acceleration according to a given operation of the end-effector. The motion laws generated by trajectory planner have to use some particular strategies to eliminate extra movements such as chattering and resonance. They have to be smooth enough, and continuous for their first and second derivatives[10,11]. Within a number of planning algorithms, cycloidal motion is especially suitable to apply in point-to-point trajectory planning because of its smaller amount of calculation, smoothness and continuity, and features of zero velocity and acceleration at the initial and end points of the bounded interval[12]. Its motion curve can be described as[13]:

$$s(\tau) = \tau - \frac{1}{2\pi}\sin 2\pi\tau \tag{14}$$

Then its first and second derivatives can be expressed as:

$$s'(\tau) = 1 - \cos 2\pi\tau \tag{15}$$

$$s''(\tau) = 2\pi \sin 2\pi\tau \tag{16}$$

where $\tau = \frac{t}{t_f - t_0} = \frac{t}{T}$, τ is normalized time; T is a single harvest operation time.

Figure 4 shows the curves of the cycloidal motion and its first and second derivatives in canonical interval (-1, 1). From Figure 4, it can be clearly seen that the cycloidal motion is adequately smooth; also, the velocity and acceleration motions are continuous and the values at the initial and end points of interval $0 \leqslant \tau \leqslant 1$ are zeros. This demonstrates that the motion of the end-effector of robot manipulator won't result chattering, so it can ensure motion stability of the robot system.

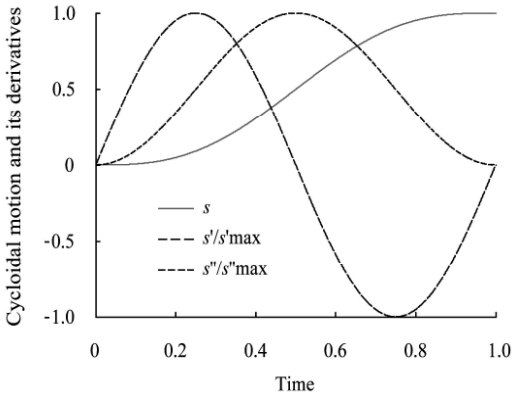

Figure 4 Cycloidal motion and its first and second derivatives

For joint i, trajectory planning relies on position and orientation of end-effector. So, the first step of trajectory planning is acquiring the three dimensional space description of the target cucumber. This description is based on sensory information such as machine vision as well as priori knowledge about kinematics structure of robot manipulator. Then the goal angles $q_i(f)$ of the four joints can be obtained from the target position of the end-effector with inverse kinematics (Eqs 6, 10, 12, 13). After the start joint angles $q_i(0)$ being sent from joint controllers through CAN-bus, the position, velocity, acceleration equations based on cycloidal motion can be expressed as:

$$q_i(t) = q_i(0) + (q_i(f) - q_i(0))s(\tau) \tag{17}$$

$$\dot{q}_i(t) = \frac{q_i(f) - q_i(0)}{T} s'(\tau) \tag{18}$$

$$\ddot{q}_i(t) = \frac{q_i(f) - q_i(0)}{T^2} s''(\tau) \tag{19}$$

6 Hardware and software design of trajectory planning based on CAN-bus

6.1 Interface circuit of CAN-bus

Controller Area Network (CAN) is an advanced serial communication protocol for distributed real-time control system. Different devices such as processors, sensors and actuators can be connected to CAN-bus via twisted-pair wires and can communicate with each other by exchanging messages. The maximum transmission rate can reach up to 1Mbps in a noisy environment. And it utilizes Carrier Sense Multiple Access with Collision Detection (CSMA/CD) as the arbitration mechanism to enable its attached nodes to have access to the bus[14-16].

The cucumber harvesting robot system employs the point to multi-points communication of CAN-bus. The upper monitor and four joint controllers are composed of dsPIC30f4012 digital signal processor which contains standard CAN controller and MCP2551 transceiver. And a 4-wire interface is designed based on CAN-bus

protocol(CAN2.0A), which provides power, ground and two data lines(CAN High and CAN Low). The interface circuit of CAN-bus is shown in Figure 5. And the upper monitor circuit board is shown in Figure 6. The Baudrate of CAN-bus communication is adopted 1Mbps, and the messages transmitted consist of 2-byte identifier, 1-byte data length and 8-byte data. Messages are transmitted with a time internal of 10 ms according to the harvesting requirements. CAN-bus communication exhibits good real-time performance in practical application.

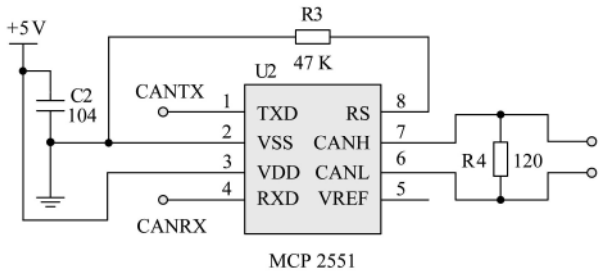

Figure 5 Interface circuit of CAN-bus

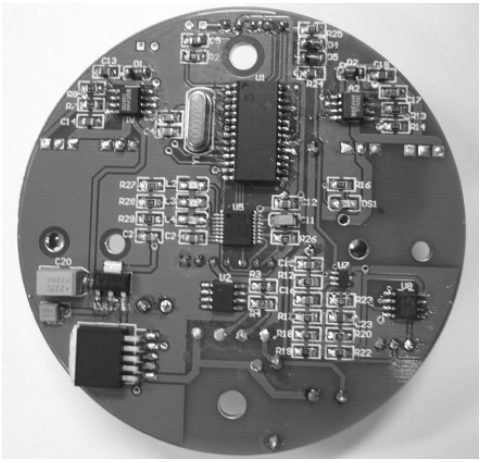

Figure 6 Upper monitor circuit board

6.2 Software design for trajectory planning of the cucumber harvesting robot

The upper monitor has functions of management and supervision for the robot system, location of cucumber target and trajectory planning. The program design employs the modularization idea which is composed of several subprograms. Figure 7 illustrates the process of the trajectory planning for the cucumber harvesting robot. It consists of subprograms such as CAN-bus sending and receiving, acquisition of cucumber target, inverse kinematics and trajectory planning.

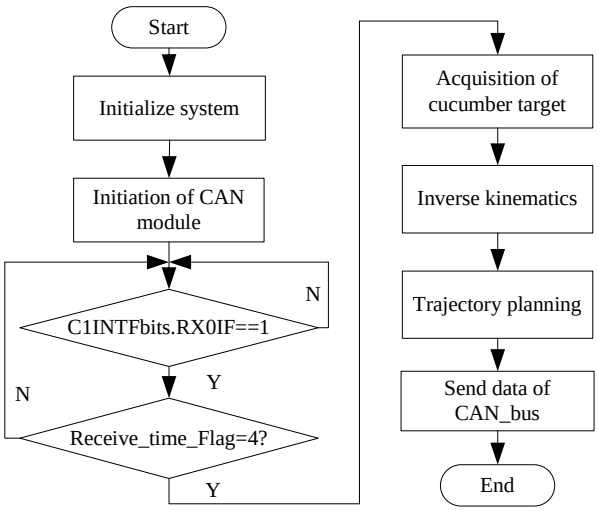

Figure 7 Flow chart for the trajectory planning

7 Experiments and analysis

In order to verify the accuracy of the trajectory planning algorithm and CAN-bus communication, experiments to measure the actual position of the four joints of the cucumber harvesting robot manipulator were performed with the coordinate measurement machine (CMM) Platinum FaroArm of FARO Technologies Incorporation. As the world's best-selling portable measurement arm, Platinum FaroArm is available in sizes ranging from 1.2 m to 3.7 m and has precision of up to 0.013 mm.

Experiments were carried out as follows:

1) Set the position of the end-effecor: p_x =700 mm, p_y =200 mm, p_z =668 mm. By utilizing the inverse kinematics, the four joint angles can be computed from equation (6) ~ (13): $\theta_1 = 15.95°$, $\theta_2 = 55.82°$, $\theta_3 = -33.48°$, $\theta_4 = -22.34°$.

2) Plan trajectories for each joint with cycloidal motion algorithm and send the planned angle messages to joint controllers by CAN-bus.

3) Use Platinum FaroArm to measure the actual angles that torque motors have rotated.

4) Set other 9 positions of end-effector, repeat (1)~(3) steps. Experimental results are presented in Table 2.

Experimental results indicate that the integrated errors of four joint angles didn't exceed four degrees. The possible reasons for experimental errors are: (1)

controlling precision of single joint is 0°～1°; (2) mechanical structure error including installation and deformation error; (3) the end-effector hadn't realized closed-loop position control. The corresponding solutions are: (1) add some compensation algorithm to improve control precision of single joint; (2) substitute Aluminum alloy for PVC to manufacture the manipulator to decrease mechanical error; (3) mount a mini camera on the end-effector to realize the close-loop control of manipulator.

Table 2 Experimental results on measuring actual position of the four joints of robot manipulator

	Theoretical values(deg)				Measured values(deg)			
	θ_1	Θ_2	Θ_3	Θ_4	θ_1	Θ_2	Θ_3	Θ_4
1	15.95	55.82	-33.48	-22.34	16.38	54.90	-33.44	-24.43
2	28.07	63.81	-37.10	-26.70	27.67	63.28	-36.55	-24.24
3	21.80	8.58	-42.63	34.05	22.59	6.19	-42.59	34.05
4	-14.04	3.98	-34.47	30.49	-14.45	1.64	-34.42	29.77
5	33.69	52.00	-35.12	-16.88	33.82	51.71	-36.47	-14.75
6	-26.57	55.70	-52.40	-3.30	-26.47	54.78	-51.55	-5.89
7	19.49	69.08	-55.16	-13.92	18.89	69.07	-54.63	-11.12
8	-12.53	4.98	-53.57	48.58	-13.34	3.85	-52.50	48.39
9	17.99	11.37	-44.42	33.05	17.76	9.18	-44.47	31.58
10	26.57	36.82	-40.87	4.05	26.23	34.90	-40.49	3.18

8 Conclusions

1) Kinematics of the cucumber harvesting robot manipulator was constructed using D-H coordinate frame model. The inverse kinematics, which provides a foundation for trajectory planning, has been solved with inverse transform technique.

2) The cycloidal motion, which has properties of continuity, small amount of calculation, and zero velocity and acceleration at the ports of the bounded interval, is proposed as a feasible approach to plan trajectory in joint space of the robot manipulator.

3) Software and hardware of CAN-bus communication between the upper monitor and the joint controllers have been designed.

4) Experimental results show that the upper monitor communicated with four joint controllers efficiently by the CAN-bus, and the integrated errors of four joint angles were less than four degrees.

Acknowledgment

This work is supported by the Natural Science Foundation of China (50575206) and the National High-Tech Research and Development (863) Program of China (2007AA04Z222).

[References]

[1] Tang Xiuying, Zhang Tiezhong. Robotics for fruit and vegetable harvesting: a review. Robot, 2005; 27(1): 90－96.

[2] E. J. Van Henten, J. Hemming, B.J.A Van Tuijl et al. Collision-free motion planning for a cucumber picking robot. Biosystems Engineering, 2003; 86(2): 135－144.

[3] Arima S, Kondo N. Cucumber harvesting robot and plant training system. Journal of Robotics and Mechatronics, 1999; 11(3): 208－212.

[4] Xiong Youlun. Robotic technology. Wuhan: Huazhong University of Science and Technology Press, 1996; pp. 18－22.

[5] M.Abderrahim, A.R.Whittaker. Kinematic model identification of industrial manipulator. Robotics and Computer Integrated Manufacturing, 2000; 16: 1－8.

[6] Chen Ning, Jiao Enzhang. A new scheme for solving the inverse kinematics equations of PUMA robot manipulator. Journal of Nanjing Forestry University. 2003; 27(4): 23－26.

[7] Fu Jingxun. Robotics. Beijing: China Science and Technology Press, 1989; pp.26－36.

[8] Wang Ping, Yang Yanping, Deng Xiao. Study on the motion control of mold polishing robot system. China Mechanical Engineering, 2007; 18(20): 2422－2424.

[9] Anatoly P. Pashkevich, Alexandre B. Dolgui. Kinematic aspects of a robot-positioner system in an arc welding application. Control Engineering Practice, 2003; 11: 633－647.

[10] Neelam R Prakash, Kamal T S. , Intelligent planning of trajectories for pick-and-place operations. In: Proc. of International Conference on System, Man and Cybernetics. 2000; 55－60.

[11] A. Gasparetto, V. Zanotto. A new method for smooth trajectory planning of robot manipulators. Mechanism and Machine Theory, 2007; (42): 455－471.

[12] Zhuang Peng, Yao Zhengqiu. Trajectory planning of suspended-cable parallel robot based on law of cycloidal motion. Mechanical Design, 2006; (9): 21－24.

[13] Jorge Angeles. The principle of robotic mechanic system. Beijing: Mechanical Industry Press, 2004; 141－148.

[14] Hofstee J W, Goense D. Simulation of a CAN-based tractor implement field bus according to DIN 9684. Journal of Agricultural Engineering Research, 1999; 73(4): 383－394.

[15] Yang Xianghui. Industrial communication and control network. Beijing: Tsinghua University Press, 2003. pp. 84－85.

[16] Navet N, Song Y Q. Reliability improvement of the dual-priority protocol under unreliable transmission. Control Engineering Practice, 1999; (7): 975－981.